# Supporting Information

# Highly selective hydrocracking of polypropylene to gasoline-range fuel over Pt/MCM-22 catalyst

*Jiawei Xu[a,b], Huijuan Han[a], Yumeng Zhao[b], Qilu Li[b], Rongyu Yang[b], Yuhan Yang[a], Hao Xu[c], Shichao Han[b,*], Xiaomin Tang[d,*], Longfeng Zhu[a,*], Qinming Wu[e], and Jiusheng Li[b]*

[a] College of Biological, Chemical Science and Engineering, Jiaxing University, Jiaxing 314001, China

[b] Shanghai Advanced Research Institute, Chinese Academy of Sciences, Shanghai 201210, China

[c] Zhejiang Collaborative Innovation Center for Full-Process Monitoring and Green Governance of Emerging Contaminants, College of Biology and Environmental Engineering, Zhejiang Shuren University, Hangzhou 310015, China

[d] *State Key Laboratory of Magnetic Resonance Spectroscopy and Imaging, Innovation Academy for Precision Measurement Science and Technology, Chinese Academy of Sciences, Wuhan 430071, China*

[e] College of Chemical and Biological Engineering, Zhejiang University, Hangzhou 310027, China

**Materials**

Polypropylene (PP, melt flow index: 4 g/10 min, Aladdin Chemistry Co., Ltd.; PP, melt flow index: 3.5 g/10 min, Titan Scientific Co., Ltd.; PP, melt flow index: 32 g/10 min, shanghai SECCO Petrochemical Co., Ltd.), zeolites were bought from Nankai University Catalyst Co., Ltd., including MCM-22, ZSM-5, Beta, FER, MOR, ZSM-22 , MCM-41, and Y, *n*-tetradecane ($C_{14}H_{30}$, GC, 99%, Shanghai Adamas Reagent Co., Ltd.), *n*-octacosane ($C_{28}H_{58}$, RG, 99%, Shanghai Adamas Reagent Co., Ltd.), chloroplatinic acid ($H_2PtCl_6 \cdot 6H_2O$, RG, 99.9%, Shanghai Adamas Reagent Co., Ltd.), ruthenium(III) chloride ($RuCl_3 \cdot xH_2O$, RG, 99.95%, Shanghai Adamas Reagent Co., Ltd.), nickel(II) nitrate ($Ni(NO_3)_2 \cdot 6H_2O$, AR, 98%, Sinopharm Chemical Reagent Reagent Co., Ltd.), palladium(II) nitrate ($Pd(NO_3)_2 \cdot 2H_2O$, AR, Sinopharm Chemical Reagent Reagent Co., Ltd.).

**Characterizations**

X-ray diffraction (XRD) data of the samples were collected with a Rigaku Ultimate VI X-ray diffractometer (40 kV, 40 mA) using CuKα radiation (λ=1.5406 Å). Scanning electron microscopy (SEM) experiments were conducted on a JEOL JSM-7401F electron microscope. Scanning transmission electron microscopy (STEM) and energy dispersive spectroscopy (EDS) elemental maps were conducted on a JEOL JSM-2100F transmission electron microscope. $N_2$ sorption isotherms at the temperature of liquid nitrogen were measured using Micromeritics Autosorb-iQ. $NH_3$ temperature-programmed desorption ($NH_3$-TPD) was performed on a fully automatic instrument (McKenna Instruments AutoChem 2920). 100 mg of the sample (20-40 mesh) was placed into a quartz tube and pretreated in a He flow at 400 °C for 30 min. The temperature was then reduced to 50 °C for $NH_3$ adsorption in a He gas mixture flow (30 mL/min) for 1 h. After saturation, the catalyst was purged by a He gas flow (30 mL/min) for 1 h to remove physically adsorbed $NH_3$ on the surface. Finally, the signal of $NH_3$ desorption was monitored by a thermal conductivity detector (TCD) with the sample heating from 50 to 600 °C at a rate of 10 °C/min under a He flow. The fourier transform infrared spectra of adsorbed pyridine (Py-IR) were measured on a Thermo Fisher Nicolet 380 spectrometer. The sample was activated at 400 °C under vacuum for 1 h, followed by adsorbing pyridine vapor at 30 °C for 1 h. Then the adsorbed pyridine was degassed at 150 °C and 350 °C for 1 h, respectively. X-ray photoelectron spectroscopy (XPS) measurements were performed on a Thermo

Scientific ESCALAB 250Xi photoelectron spectrometer with Al Kα radiation. The binding energy was calibrated by the C *1s* peak at 284.8 eV. The compositions of the samples were determined by Perkin-Elmer Avio 200 inductively coupled plasma optical emission spectrometer (ICP-OES). Thermogravimetric analysis (TGA) was performed on a TGA 55 (TA Instruments) on flow of air or $N_2$ from room temperature to 800 °C at a heating rate of 10 °C/min. The melting points of PP and the solid residues were measured by Mettler Toledo DSC 3/500. The liquid was obtained and analyzed with a gas chromatography-mass spectrometry (Thermo Fisher Scientific Trace1310+ISQ) equipped with a flame ionization detector (FID) and HP-5 column (30 m × 0.32 mm × 0.25 μm).

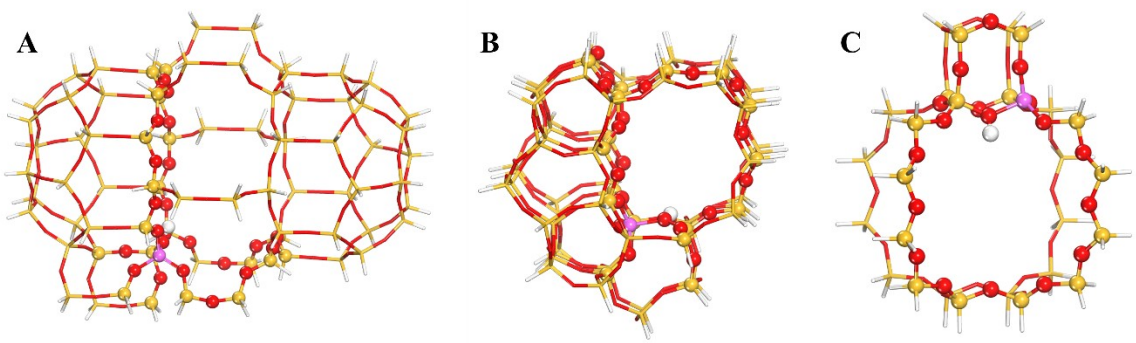


**Figure S1**. Initial structures of (A) H-MWW, (B) H-MFI, and (C) H-BEC, respectively. The structures adopted the ONIOM model, in which the higher-level atoms were represented by spheres and the lower-level atoms by sticks. Si, Al, O and H atoms are displayed in yellow, pink, red and white, respectively.

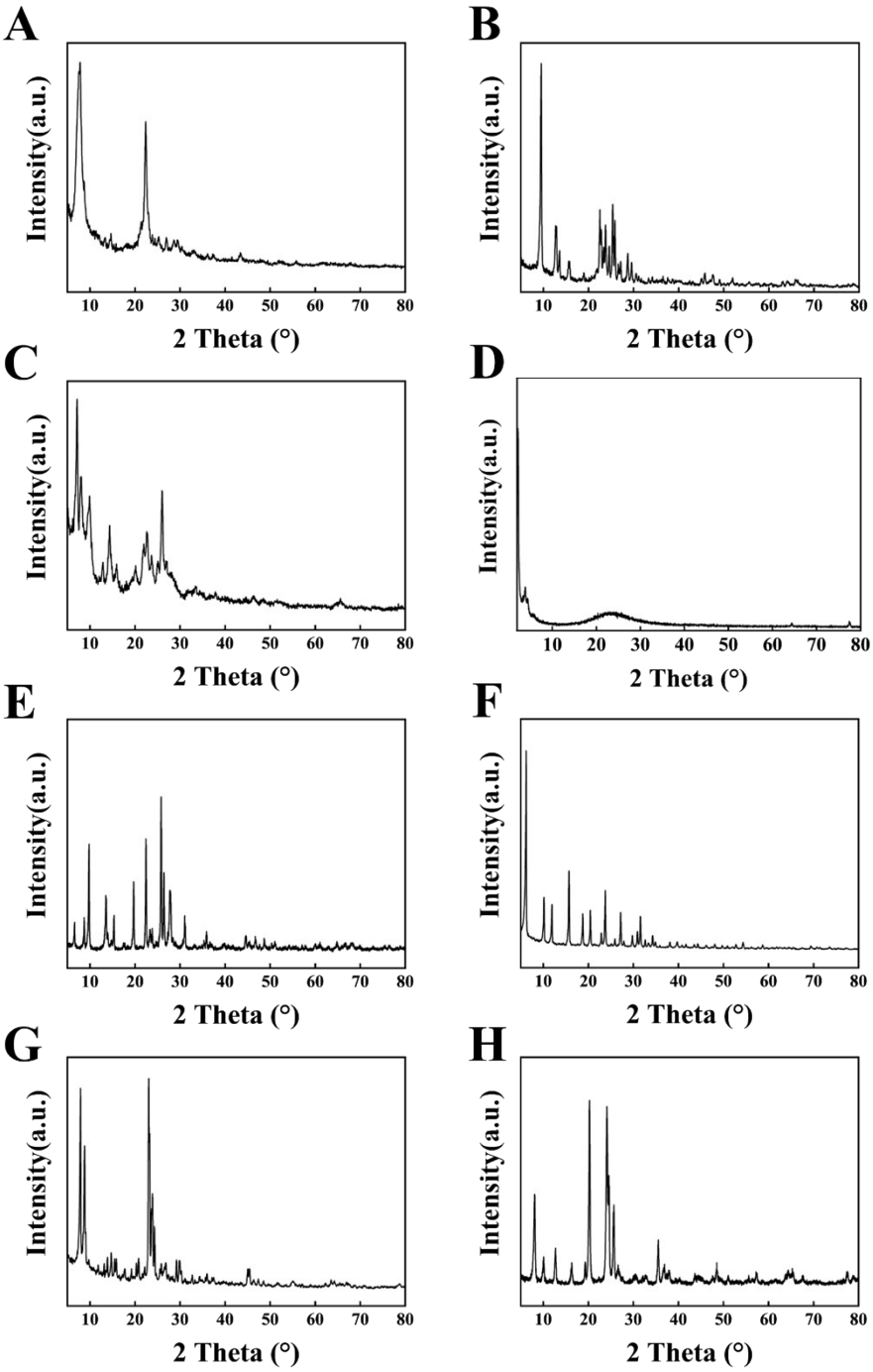


**Figure S2**. XRD patterns of (A) Pt/Beta, (B) Pt/FER, (C) Pt/MCM-22, (D) Pt/MCM-41, (E) Pt/MOR, (F) Pt/Y, (G) Pt/ZSM-5, and (H) Pt/ZSM-22 catalysts.

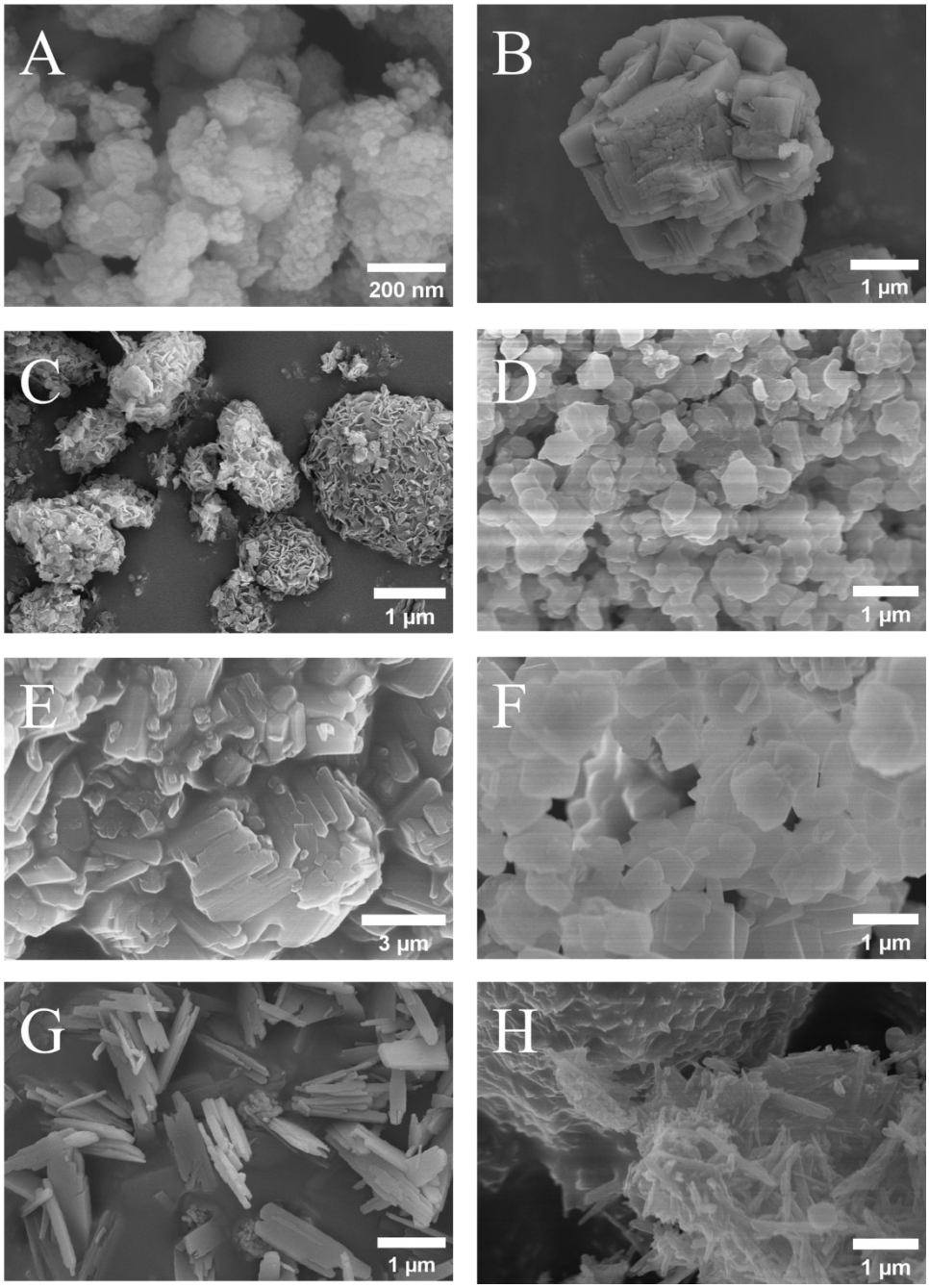


**Figure S3**. SEM images of (A) Pt/Beta, (B) Pt/FER, (C) Pt/MCM-22, (D) Pt/MCM-41, (E) Pt/MOR, (F) Pt/Y, (G) Pt/ZSM-5, and (H) Pt/ZSM-22 catalysts.

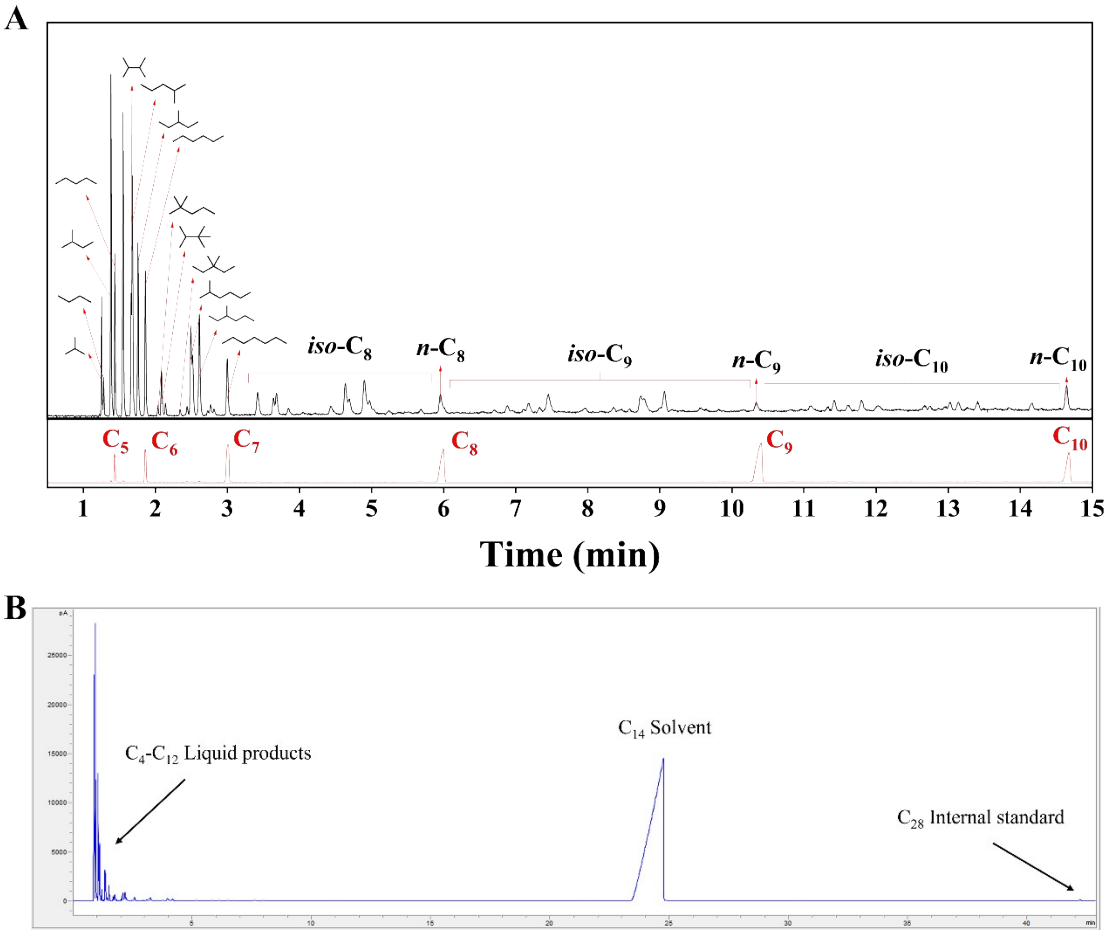


**Figure S4**. (A) GC-MS and (B) GC analysis of liquid products ($C_4$-$C_{10}$) from the catalytic PP upcycling using *n*-alkanes as the reference standard.

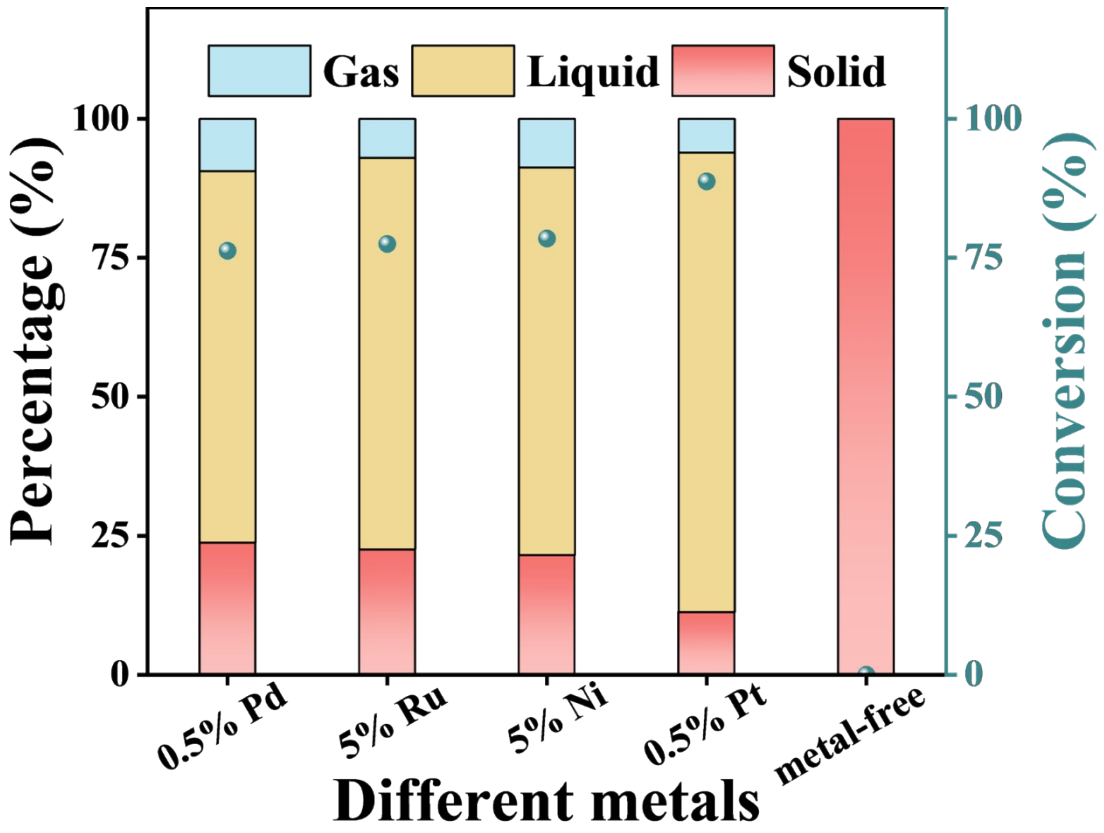


**Figure S5**. PP hydrocracking over different metal-based MCM-22 catalysts. Reaction condition: 275 °C, 3 MPa $H_2$, 4 h, 15 g PP, and 0.75 g catalyst.

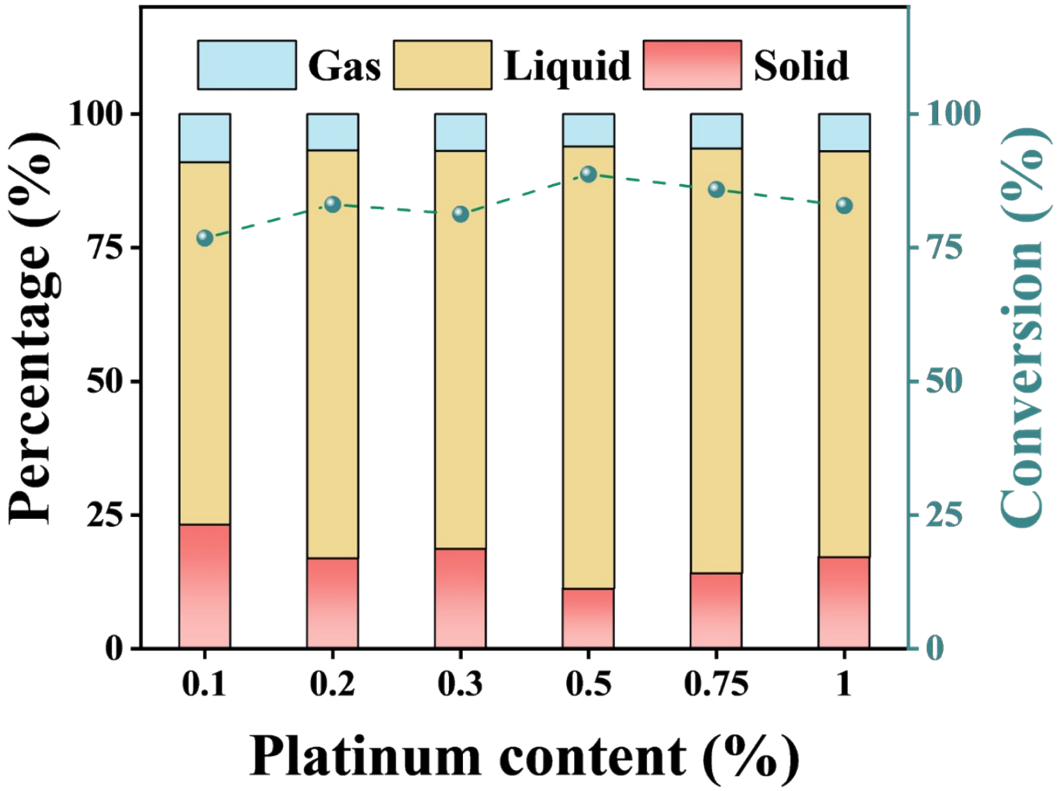


**Figure S6**. PP hydrocracking over Pt/MCM-22 catalysts with different Pt contents. Reaction condition: 275 °C, 3 MPa $H_2$, 4 h, 15 g PP, and 0.75 g catalyst.

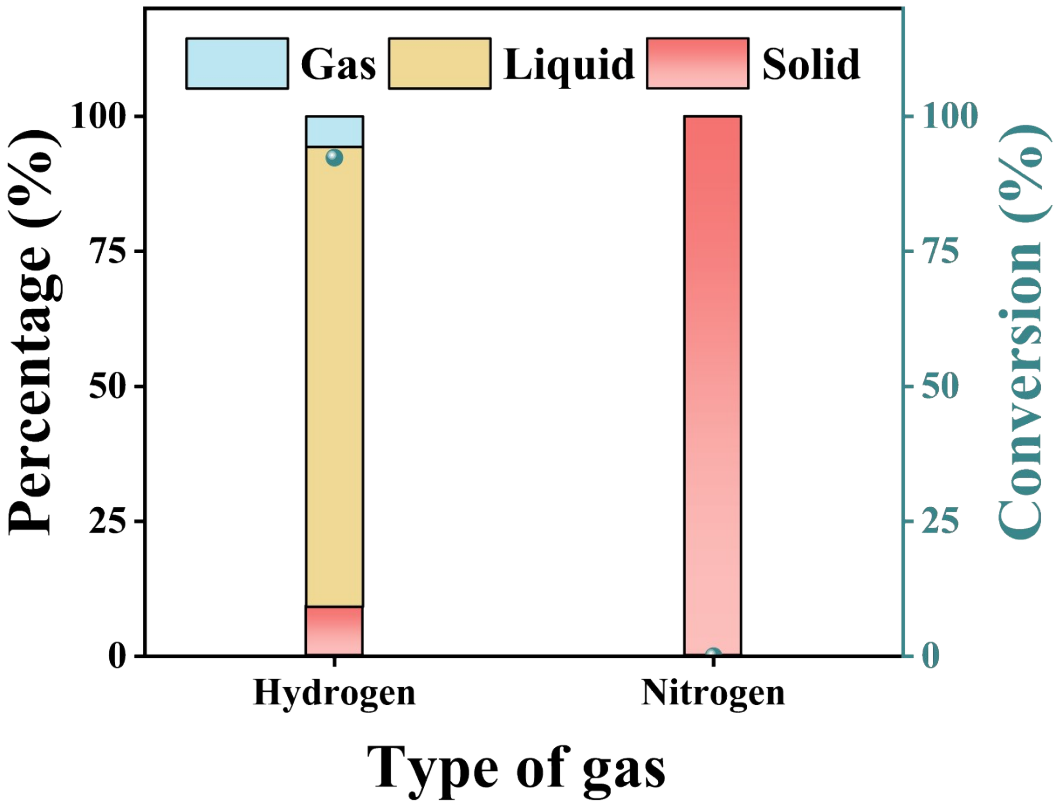


**Figure S7**. PP cracking over Pt/MCM-22 catalysts under $H_2$ or $N_2$ atmosphere. Reaction conditions: 275 °C, 3 MPa pressure, 4 h, 15 g PP, and 0.75 g catalyst.

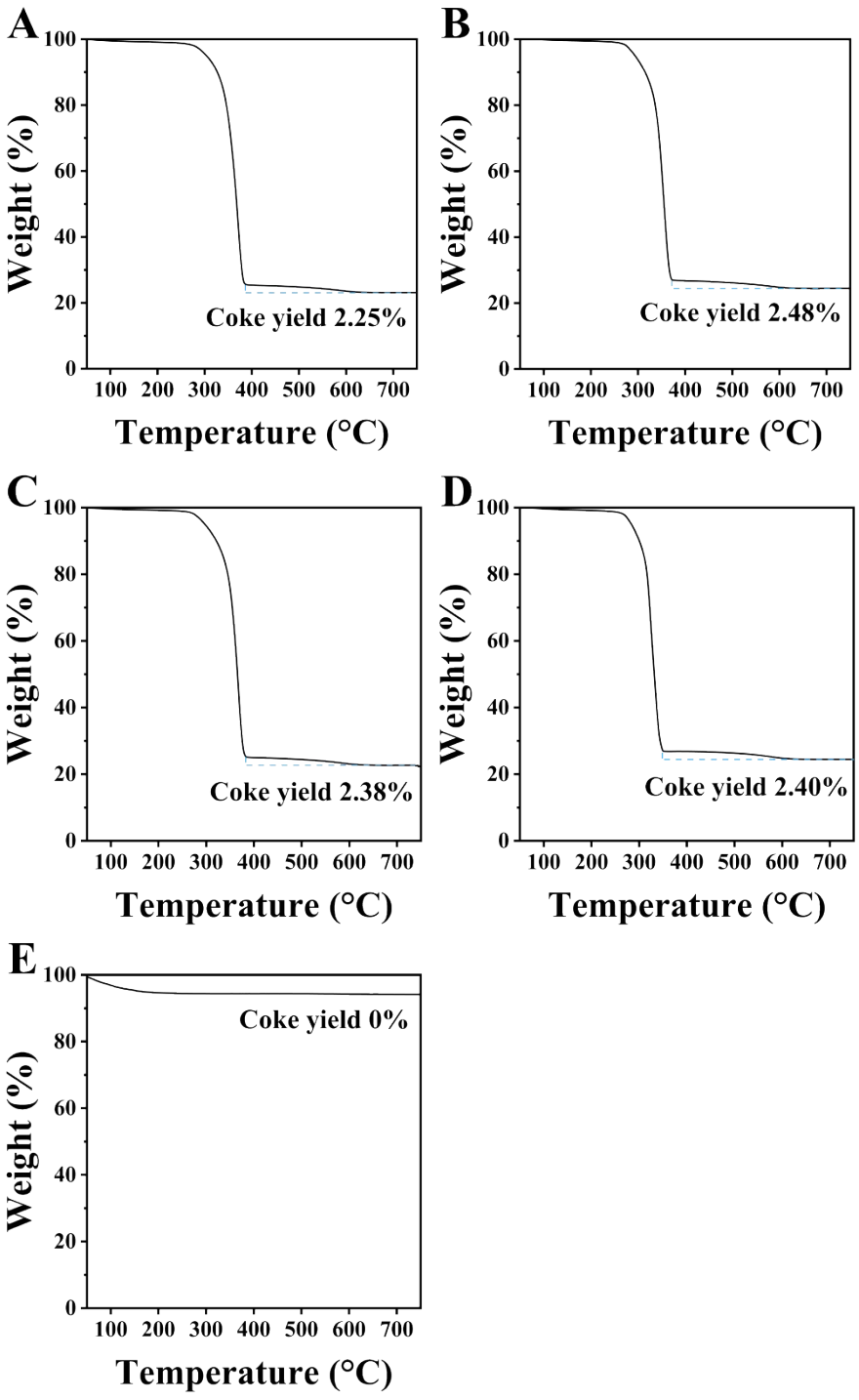


**Figure S8**. TGA curve of catalysts used after (A) 1, (B) 2, (C) 3, (D) 4 cycles, and (E) catalyst regenerated under air conditions.

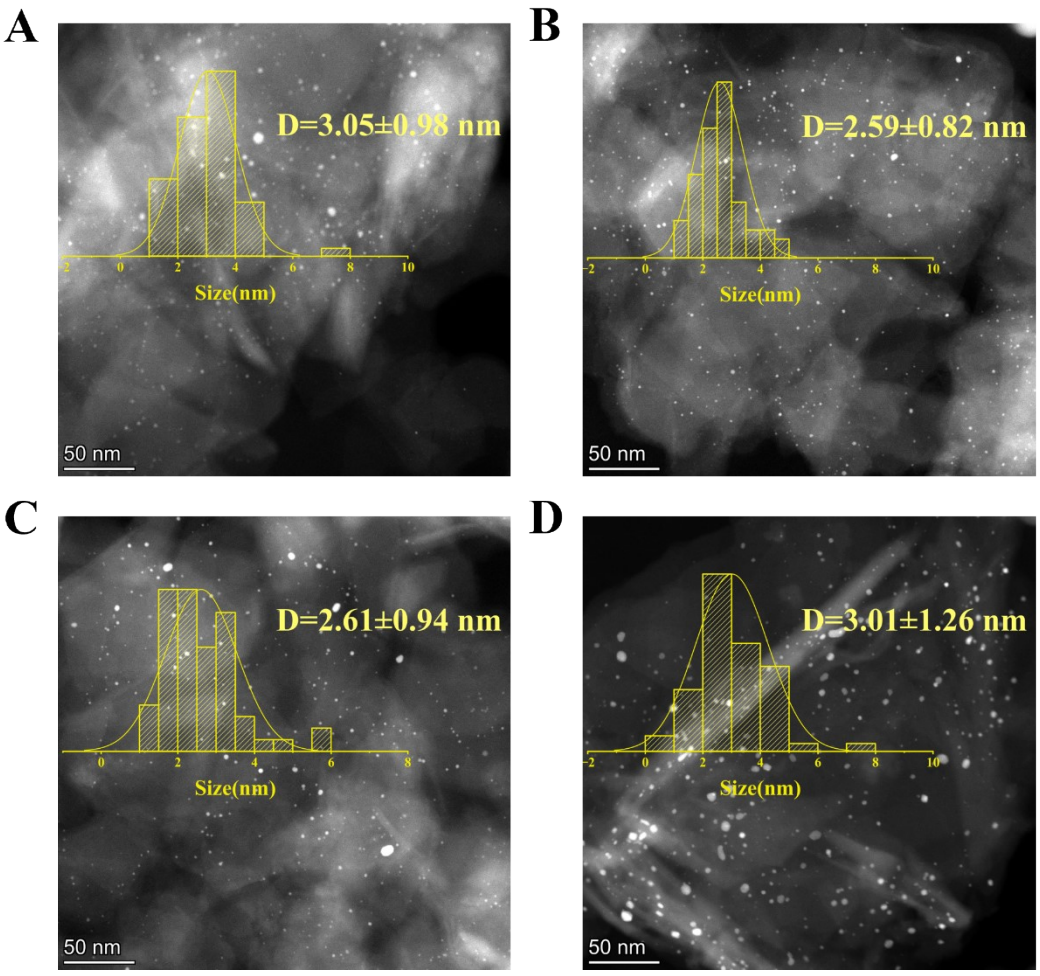


**Figure S9**. STEM images of catalysts used after (A) 2, (B) 3, and (C) 4 cycles, and (D) catalyst regenerated under air conditions.

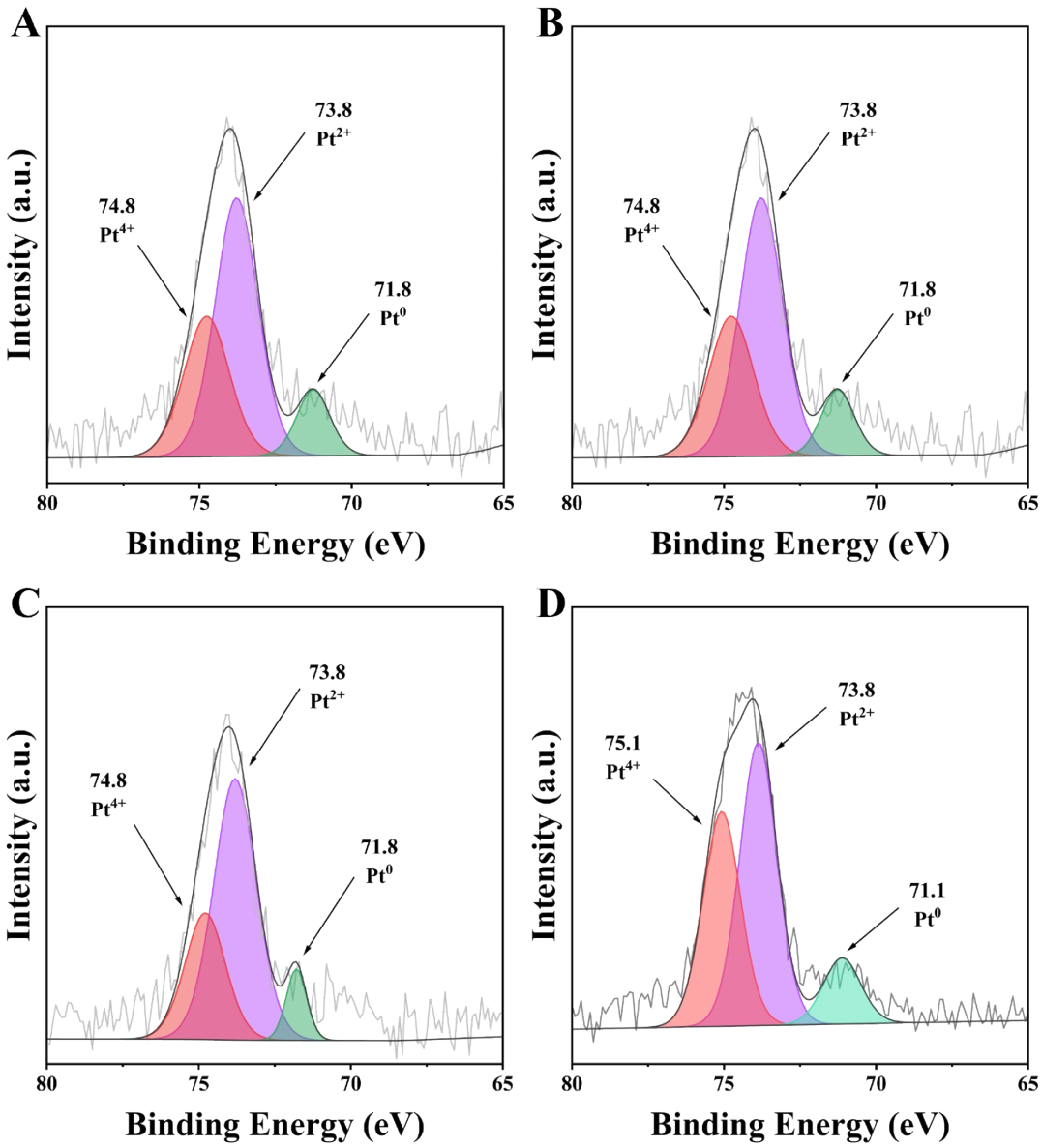


**Figure S10**. XPS spectra of catalysts used after (A) 2, (B) 3, and (C) 4 cycles, and (D) catalyst regenerated under air conditions.

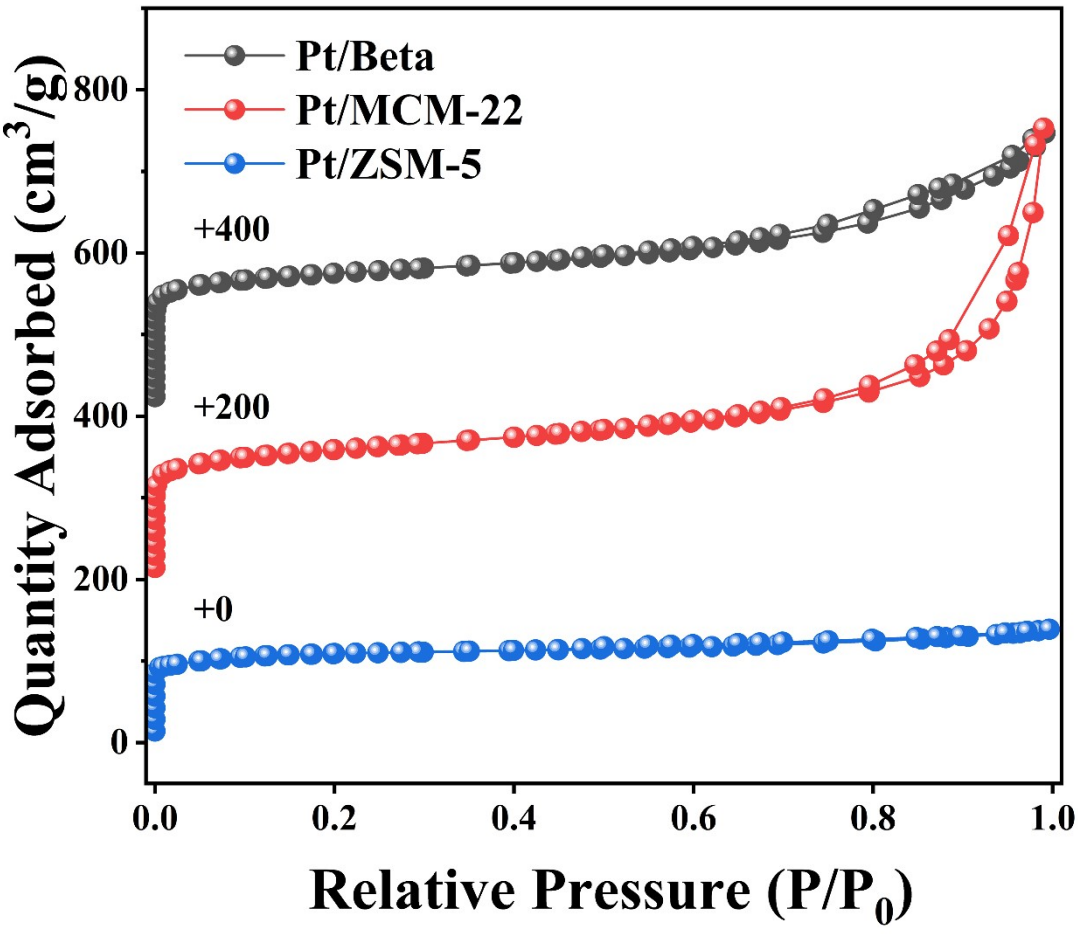


**Figure S11**. $N_2$ sorption isotherms of Pt/Beta, Pt/MCM-22 and Pt/ZSM-5 catalysts.

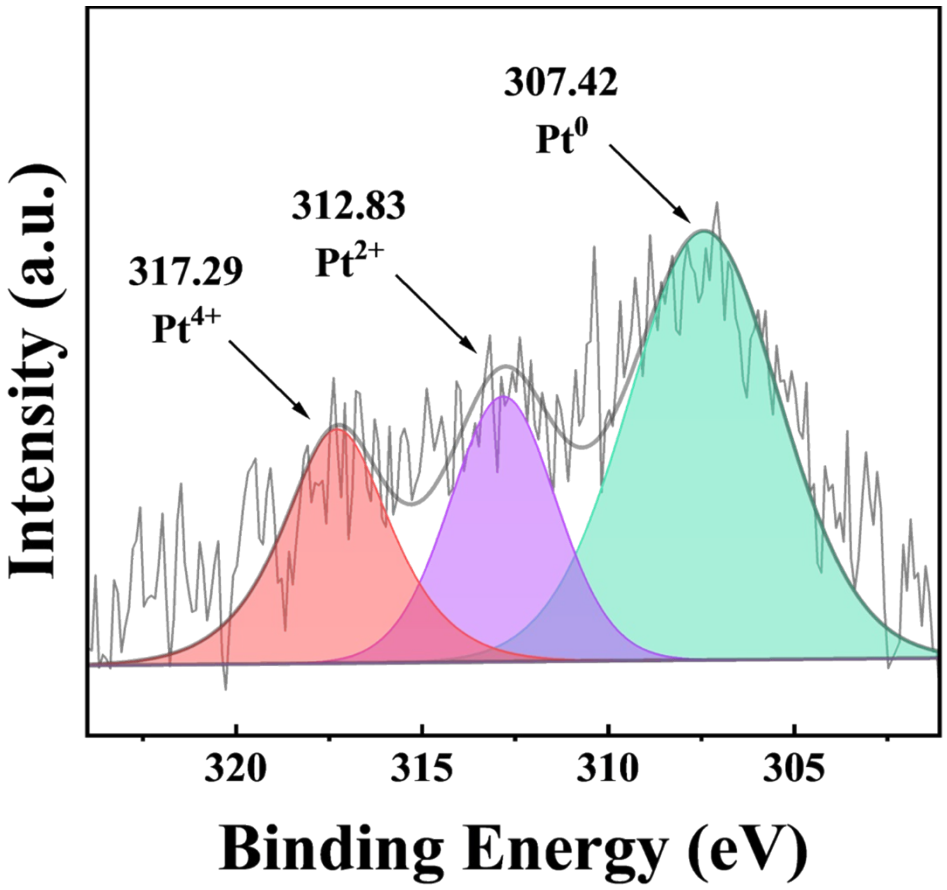


**Figure S12**. XPS spectrum of Pt/MCM-22 catalyst.

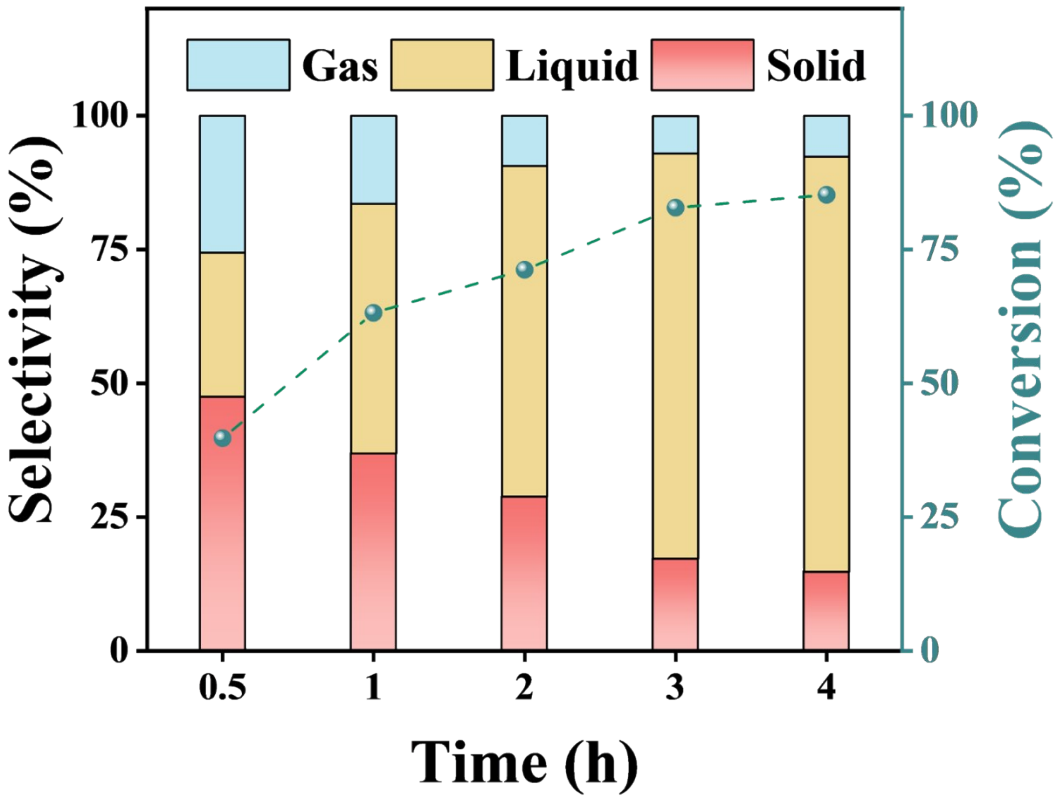


**Figure S13**. $H_2/D_2$ isotope exchange experiment of PP hydrocracking over Pt/MCM-22 at different reaction times. Reaction condition: 275 °C, 3 MPa $D_2$, 15 g PP, and 0.75 g catalyst.

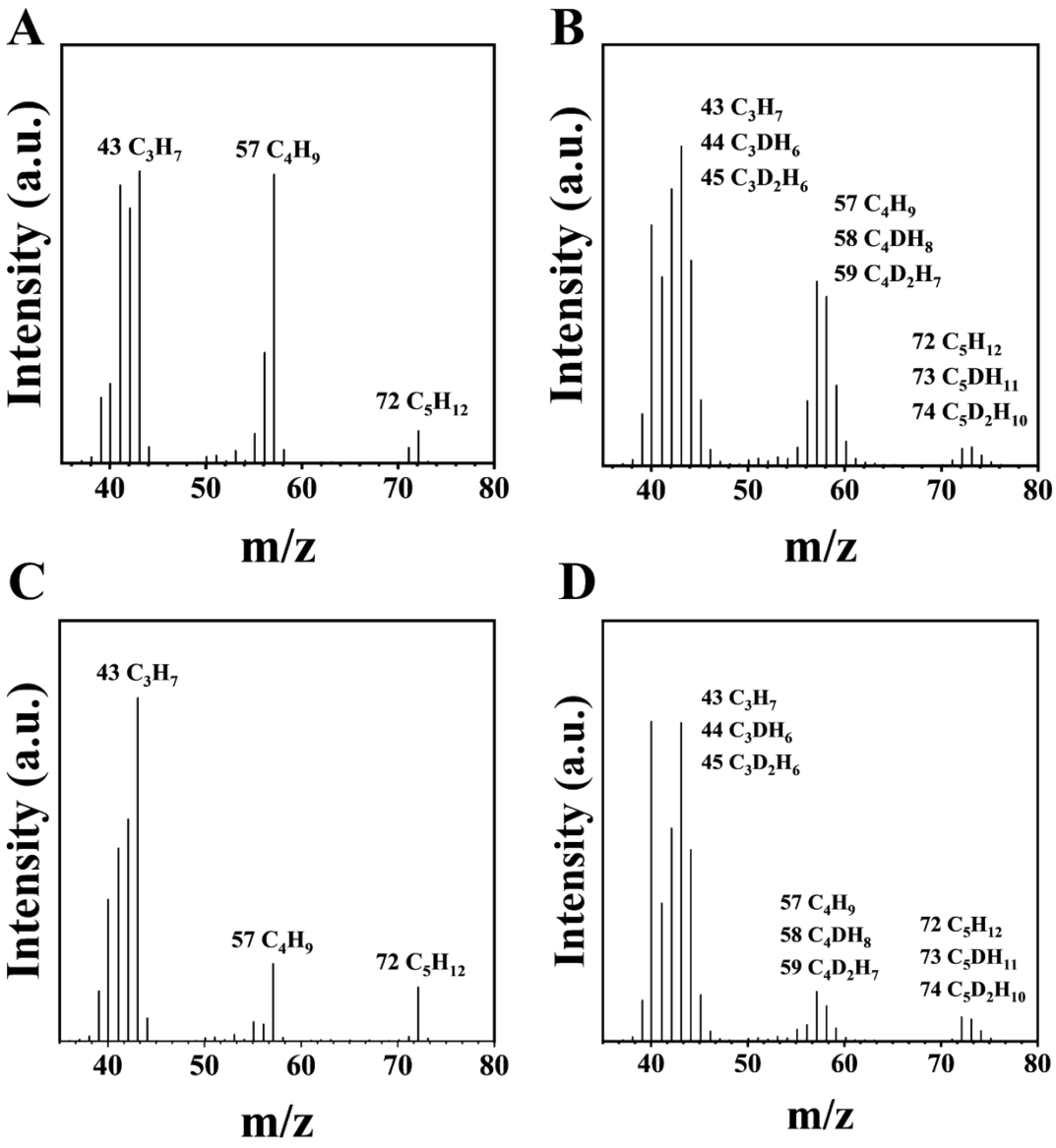


**Figure S14**. Mass spectra of (A) *i*-$C_5H_{12}$, (B) *i*-$C_5D_2H_{10}$, (C) *n*-$C_5H_{12}$, and (D) *n*-$C_5D_2H_{10}$.

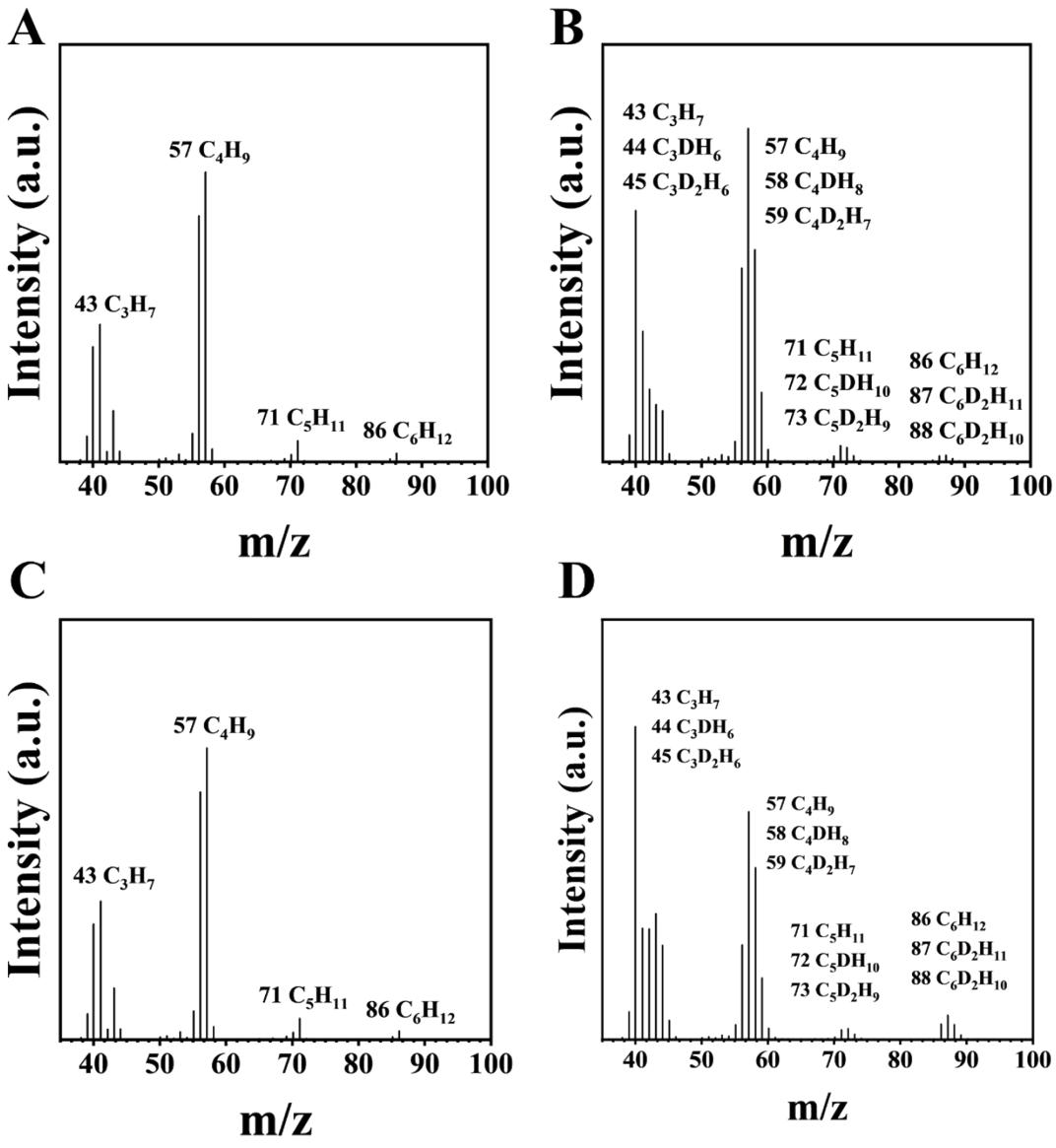


**Figure S15**. Mass spectra of (A) *i*-$C_6H_{14}$, (B) *i*-$C_6D_2H_{12}$, (C) *n*-$C_6H_{14}$, and (D) *n*-$C_6D_2H_{12}$.

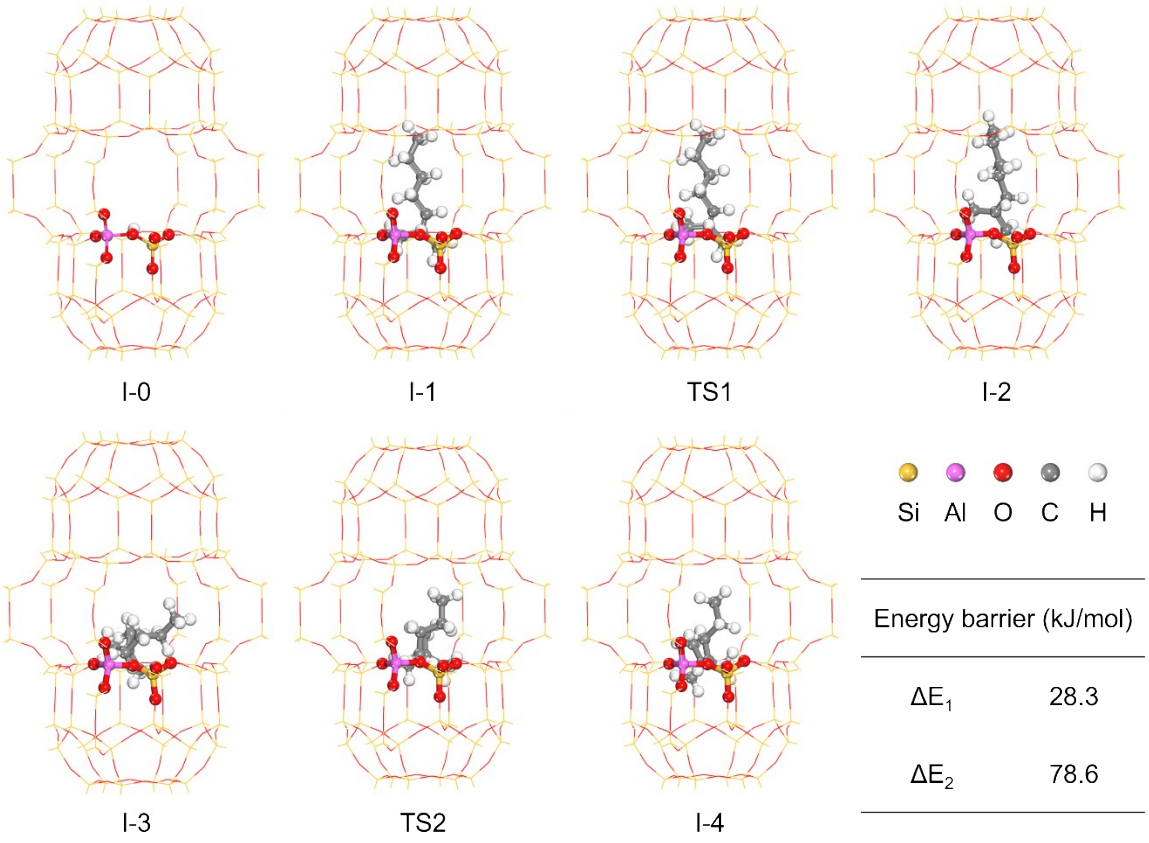


| Energy barrier (kJ/mol) | |
|---|---|
| $\Delta E_1$ | 28.3 |
| $\Delta E_2$ | 78.6 |

**Figure S16.** The optimized structures in the β-scission process on H-MWW zeolite model.

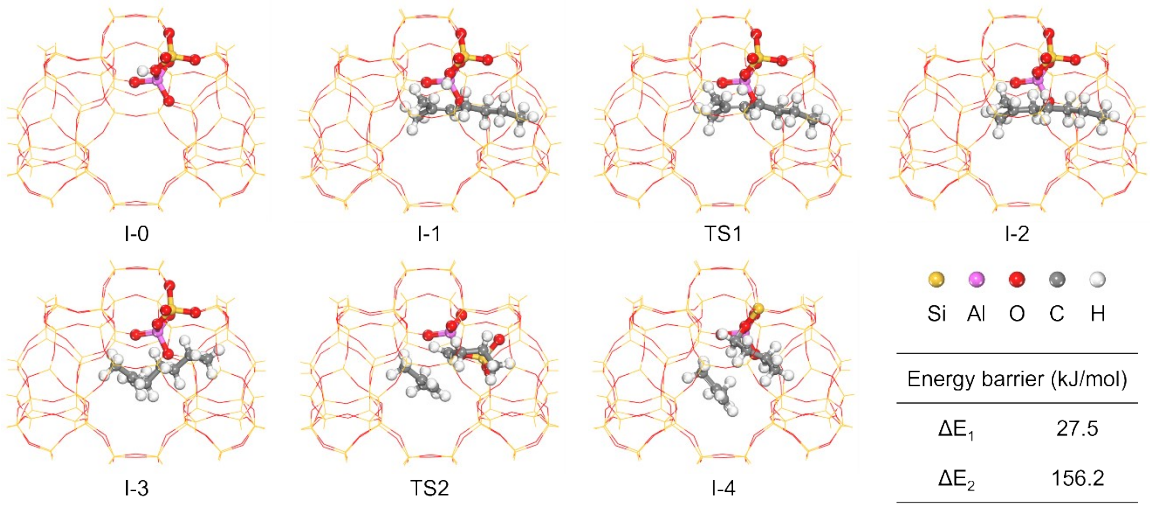


**Figure S17.** The optimized structures in the β-scission process on H-MFI zeolite model.

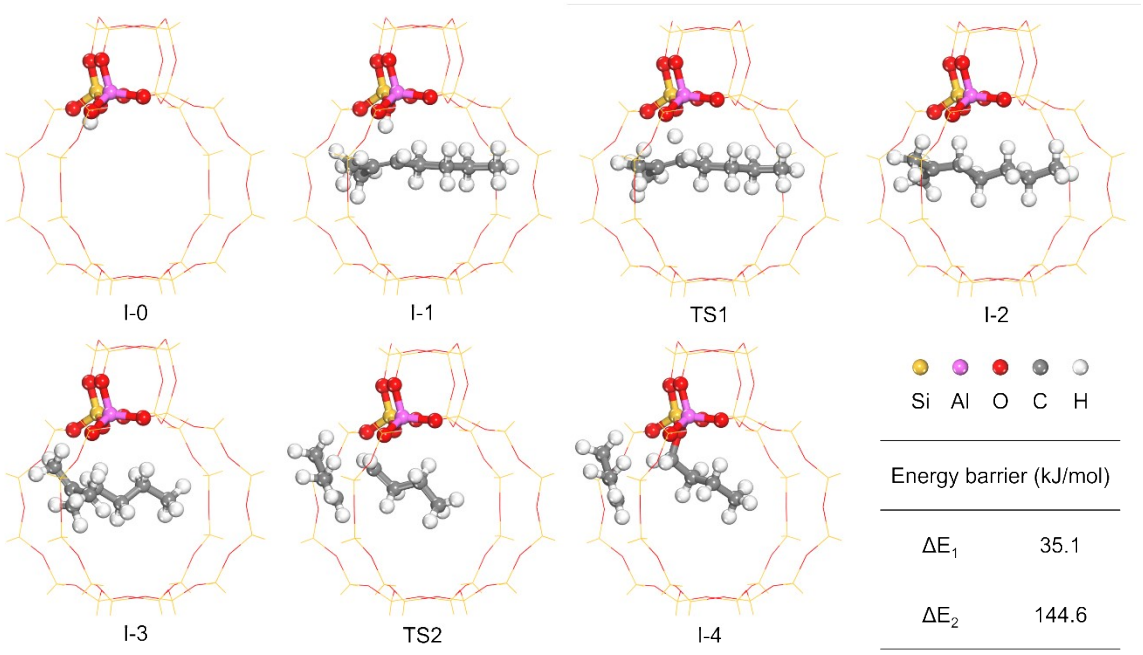


**Figure S18.** The optimized structures in the β-scission process on H-BEC zeolite model.

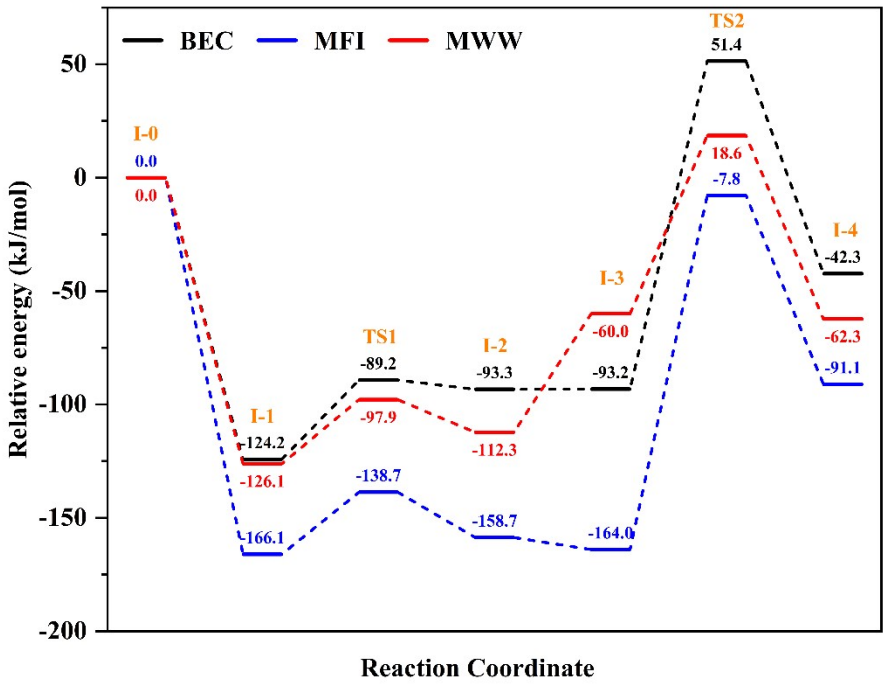


**Figure S19**. DFT calculation optimized reaction intermediates and transition states of β-scission of 2-methyl-2-heptene within MWW, MFI, and BEC frameworks, respectively.

**Table S1.** Si/Al ratios of various catalysts determined by ICP-OES.

| Samples | Si/Al ratio |
|---|---|
| Y | 3.5 |
| Beta | 10.8 |
| MCM-22 | 13.9 |
| ZSM-5 | 14.9 |
| MCM-41 | 26.2 |
| ZSM-22 | 23.3 |
| MOR | 8.7 |
| FER | 13.3 |

**Table S2.** Textural properties were determined from $N_2$ sorption.

| Samples | $A_{BET}$ ($m^2 \cdot g^{-1}$) | $A_{micro}$ ($m^2 \cdot g^{-1}$) | $A_{meso}$ ($m^2 \cdot g^{-1}$) | $V_{micro}$ ($cm^3 \cdot g^{-1}$) | $V_{total}$ ($cm^3 \cdot g^{-1}$) |
|---|---|---|---|---|---|
| Pt/Beta | 659 | 511 | 148 | 0.21 | 0.54 |
| Pt/MCM-22 | 591 | 412 | 179 | 0.17 | 0.86 |
| Pt/ZSM-5 | 414 | 370 | 44 | 0.15 | 0.22 |

**Table S3.** Summary of acidities of Pt/Beta, Pt/MCM-22 and Pt/ZSM-5. Data were determined by $NH_3$-TPD and Py-IR analyses.

| Samples | Acidity (μmol·g$^{-1}$) | | | | Total acidity[b] (μmol·g$^{-1}$) |
|---|---|---|---|---|---|
| | Brønsted acidity[a] | | Lewis acidity[a] | | |
| | 150 °C | 350 °C | 150 °C | 350 °C | |
| Pt/Beta | 14.0 | 8.8 | 118.0 | 51.4 | 1745.2 |
| Pt/MCM-22 | 26.5 | 12.7 | 85.0 | 40.8 | 1612.0 |
| Pt/ZSM-5 | 25.8 | 5.4 | 83.4 | 33.5 | 2090.0 |

[a] Determined by Py-IR technique.

[b] Determined by $NH_3$-TPD technique.